Published in final edited form as:
Electrophoresis. 2012 December ; 33(23): 3448–3457. doi:10.1002/elps.201200165.

K^+, Na^+, and Mg^{2+}on DNA Translocation in Silicon Nitride Nanopores

James Uplinger, **Brian Thomas**, **Ryan Rollings**, **Daniel Fologea**, **David McNabb**[1], and **Jiali Li**[*]

Department of Physics, University of Arkansas, Fayetteville, AR 72701

[1]Department of Biological Sciences, University of Arkansas, Fayetteville, AR 72701

Abstract

In this work we report on how salt concentration and cation species affect DNA translocation in voltage-biased silicon nitride nanopores. The translocation of double-stranded DNA (dsDNA) in linear, circular, and supercoiled forms was measured in salt solutions containing KCl, NaCl, and $MgCl_2$. As the KCl concentrations were decreased from 1M to 0.1M, the time taken by a DNA molecule to pass through a nanopore was shorter and the frequency of the translocation in a folded configuration was reduced, suggesting an increase in DNA electrophoretic mobility and DNA persistence length. When the salt concentration was kept at 1M, but replacing K^+ with Na^+, longer DNA translocation times (t_d) were observed. The addition of low concentrations of $MgCl_2$ with 1.6M KCl resulted in longer t_d and an increased frequency of supercoiled DNA molecules in a branched form. These observations were consistent with the greater counterion charge screening ability of Na^+ and Mg^{2+} as compared to K^+. In addition, we demonstrated that dsDNA molecules indeed translocated through a ~10 nm nanopore by PCR amplification and gel electrophoresis. We also compared the dependence of DNA mobility and conformation on KCl concentration and cation species measured at single molecule level by silicon nitride nanopores with existing bulk-based experimental results and theoretical predictions.

Keywords

Counterion charge screening; DNA conformation; DNA mobility; DNA translocation; Silicon nitride nanopore

1 Introduction

The binding of metal ions (cations or counterions) to negatively charged dsDNA molecules play crucial roles in DNA double helix stability and structure [1–4]. In an ionic solution, cations bind to negatively charged DNA molecules due to strong ionic interactions, and the bound counterions can partially neutralize the negative charge of DNA molecules; thereby, reducing their net or effective charge and changing their electrophoretic mobility and shape [2, 3]. The interactions of cations with DNA molecules have been studied experimentally by bulk electrophoresis-based measurements [5–9] and they have also been evaluated theoretically [4, 10–13]. These studies revealed details into how the binding of cations could neutralize the negative charges of DNA molecules, reduce their electrophoretic mobility, and affect their conformation. More recently, the interactions of cations with DNA molecules [14], negatively charged [15] and even neutral [16] polymers have also been

Corresponding Author: Jiali Li, Department of Physics, Room 226, University of Arkansas, 825 w Dickson Street, Fayetteville, AR 72701, jialili@uark.edu, Phone: (479) 575-7593. Fax: (479) 575-4580.

studied with nanopores. In this work, we use the chloride salts of three phosphate-binding metal ions K^+, Na^+, and Mg^{2+} to study their effects on DNA translocation in silicon nitride nanopores. The goal of this study was to identify the optimum salt conditions to characterize DNA molecules during the development of a solid-state nanopore-based technology as an approach for high throughput DNA sequencing.

Voltage biased nanometer size pores allow charged particles to be measured one molecule at a time and have been developed for electronic detection and analysis of single biomolecules [17–23]. Motivated by the advancing nanopore-based technology, size adjustable solid-state nanopores have been fabricated with insulating materials such as silicon nitride, silicon dioxide, and aluminum oxides [24–35]. The electric field near a voltage-biased nanopore in an ionic solution can capture a charged DNA molecule (Fig. 1A) and drive it through the pore. A DNA molecule passing through a nanopore induces a measurable transient current drop (Fig. 1E) whose amplitude (ΔI_b) and time duration (t_d) depend on the properties of the pore, solution, DNA, and the applied voltage. Our early studies on dsDNA translocation in solid-state nanopores in a solution containing 1M KCl showed that the time duration, t_d, was dependent on the pore diameter, D_p [25]. When the diameter was small, D_p<3 nm, very long t_ds were observed and it was hypothesized that the longer t_ds were the result of the interactions between a DNA and the nanopore. When the nanopore had $D_p \geq 8$ nm, the distributions of the t_ds were approximately Gaussians and the most probable peak values of t_d were inversely proportional to the applied voltage V, indicating that those DNA molecules were electrophoretically driven and passed through a nanopore "freely" (24). These observations were consistent with other recent studies that demonstrated the dependence of DNA translocation on nanopore size [36, 37].

DNA molecules are sensitive to the electrolyte environment such as salt concentration and ionic species [38]. In this work, using silicon nitride nanopores with a $D_p \geq 8$ nm, we systematically study how the concentration of KCl and cation species affects DNA translocation time t_d and DNA conformation. To increase the range of t_d and the amplitude of ΔI_b, especially at lower KCl concentrations, DNA molecules of different lengths were used, including: linear DNA of 3 kbp (~1 μm) and 48.5 kbp (~16.5 μm), circular relaxed and circular supercoiled DNA of ~4.4 kbp and 22.5 kbp. Furthermore, we demonstrated that a 1 kbp DNA fragment did indeed translocate through a ~10 nm silicon nitride nanopore using PCR amplification and agarose gel electrophoresis. We also compared our data to with existing experimental results and theoretical predictions.

2. Materials and methods

Solutions: KCl, NaCl, and $MgCl_2$ used in this study were molecular biology or ultra-pure grade. All experiments were performed in a TE buffer (10 mM Tris, 1 mM EDTA, pH=7.5) at room temperature (~22°C). The buffered solutions were filtered through Whatman 0.02 μm nucleopore filters and degased prior to use.

DNA molecules: Three forms of DNA molecules were used in this work: linear 3 kbp plasmid pSP65 [29] and 48.5 kbp λ (Fig. 1A), circular relaxed 5.4 kbp PhiX174 (RFII) (Fig. 1B), circular supercoiled (above 90% supercoiled) ~4.4 kbp pBR322 (Fig. 1C), and a mixture of circular and supercoiled 22.5 kbp pXba (~80%). Gel electrophoresis showed the pXba mixture also contained a small amount (~5%) of linear DNA, data not shown). Except where indicated, the DNA molecules were purchased from New England Biolabs. The final DNA concentration in the *cis* chamber was ~10 nM for all the measurements.

Nanopores: Nanopores were fabricated in a freestanding ~280 nm thick low stress silicon nitride membrane supported by a 380 μm thick silicone substrate. The size of the freestanding membrane was ~30×30 μm^2. The nanopores were made using a combination of focus ion beam milling and feedback controlled ion beam sculpting [24, 39, 40]. The size of nanopores was determined by Transmission Electron Microscope (TEM). Figure 1D shows a TEM image of a ~10 nm pore used for the λ DNA measurement (Fig. 1E and 1F). The thickness of the nanopores (H_p, shown in Fig. 1A) was estimated to be ~15 nm [40]. To minimize pore-to-pore variation in diameter, thickness, and surface charge, a single nanopore or multiple nanopores with approximately the same parameters were used to generate each data set.

Data acquisition: The details of measuring DNA in a solid-state nanopore were described previously [25, 29]. Briefly, a silicon nitride membrane with a nanopore (Fig. 1A) separates two salt solution-filled chambers. A constant bias voltage, Ψ=120 mV is applied to a pair of Ag/AgCl electrodes embedded in the solution. Salt solutions were exchanged by flushing both the *cis* and *trans* chambers through fluidic systems. The *cis* and *trans* chambers were cast in PDMS [29, 30]. Examples of current drop events produced by λ dsDNA are shown in Fig. 1E and Fig. 1F at 1 M and 0.2 M KCl, respectively. The current blockage events were recorded using an Axopatch 200B (Molecular Devices) in event driven and voltage-clamp mode. The low pass Bessel filter in the Axopatch 200B was set to 10 kHz or 100 kHz. The time response of the Axopatch 200B system at these filter settings was tested and calibrated with synthetic current drops: ideal square pulses of width ranging from 20 to 300 μsec generated from a function generator (Agilent 33250A) (*see* SI. 1a). When the pulse width was between 25 and 100 μs, the pulse height was attenuated, but the time durations can be measured accurately up to 25 μs under our data analysis routines as described below. The time response of a nanopore membrane was also tested at these filter settings (SI. 1b). Our analysis shows that the time response of a nanopore membrane is less than ~20 μs. Therefore, the bandwidth of the Axopatch and the membrane capacitance would not be a limiting factor for the time durations measured ($t_d \geq 50$ μs).

Analysis of current blockage events: As illustrated in Fig. 1E, current drop events are characterized by its average amplitude ΔI_b and time duration t_d. The integral of an event, referred to as the event charge deficit (*ecd*), as discussed previously [29], was also calculated. These parameters are extracted using our custom MATLAB routines (*see* SI. 3 for details), and are presented in the event distribution plots (i.e. Fig. 2A) in which each event, represented by a dot, is defined by its ΔI_b and t_d. In a distribution of events, the presences of different DNA conformations are shown in separable clusters, and the events from the same conformation (cluster) are used for comparison. As an example, the λ DNA event distribution plot shown in Fig. 2A, depicts the cluster of linear and folded translocation events [25]. The t_d and ΔI_b distributions are shown on the axes. The distributions were fitted with Gaussian functions (solid curve). A single Gaussian function was used if the event cluster is well separated or only one form of DNA was used. Two Gaussian functions were used if the events resulting from different DNA conformations were not well resolved. We used the fitted peak values, ΔI_{bp} and t_{dp}, as the most probable current drop and translocation time of the each cluster. The errors to the peak values are the standard deviations of the fittings. A table of the t_{dp} and ΔI_{bp} values for all DNA molecules at all KCl concentrations is included in table 1 for comparison.

3. Results and discussion

3.1 ΔI_b and t_d affected by KCl concentration

—As the KCl concentration was decreased from 1M to 0.2M, the event distribution plots (Fig. 2), ΔI_b versus t_d, show signature patterns of DNA translocation in solid-state nanopores. For the λ DNA in 1M KCl, the event distribution (Fig. 2A) shows a constant *ecd* = ($\Delta I_{bp} \cdot t_{dp}$), best fit to $\Delta I_b = ecd/t_d$, consistent with our previously published results for linear dsDNAs [25, 29, 41]. For the linear translocation events, defined as N=1, where N is the number of double-stranded helices in the pore, the most probable values were ΔI_{bp}~104 pA and t_{dp}~2.94±0.32 ms. For the folded or N=2 events, with two helices in the pore, the values were found to be ΔI_{bp} ~180 pA and t_{dp}~1.60±0.26 ms. In contrast, at 0.2M KCl, the event distribution did not show a clear separation between the N=1 and N=2 events as compared to 1M KCl. The most probable values measured were ΔI_{bp}~28 pA and t_{dp} ~ 0.57±0.04 ms.

For the circular form of DNA (22.5 kbp pXba) in 1 M KCl, the event distributions show that the ΔI_{bp} ~220 pA (on the left axis of Fig. 2B), approximately twice the value of ΔI_{bp} for N=1 λ DNA. This was expected since circular DNA must translocate with two helices in the pore (N= 2). For the pXba in a supercoiled form, the ΔI_b was larger as the t_d was shorter as a result of the increased number of superhelical turns [41]. For the 4.4 kbp pBR322 DNA (≥ 90% in circular supercoiled form), the distribution of current blockage events were fit to single Gaussians. The short time durations, t_d ~430 μs for the pXba (Fig. 2B) and t_d ~ 100 μs for the pBR322 (Fig. 2C) in 1M KCl, were due to their shorter lengths. The small difference in ΔI_b for N=2 could be the result of possible geometric differences along the length of the nanopores used for these two sets of measurements.

The data in Figure 2 demonstrated that as the KCl concentration was lowered, smaller ΔI_b were observed. The much smaller ΔI_b~20pA for the long (~16.5 μm) linear λ DNA at 0.2M KCl (Fig. 1F) is clearly seen in the recorded data traces compared with the events recorded in 1M KCl (Fig. 1E). These event distributions show that: 1) the ΔI_b is approximately proportional to the KCl concentration or solution conductivity and the number of strands (N) in a pore; and 2) t_d is longer for longer DNA molecules. These observations were consistent with the fact that the DNA molecules were electrophoretically translocated through the nanopores during the measurements.

The previously reported positive spikes seen with SiO_2 pores were not observed: The positive spikes at low salt concentrations (<0.4M) reported by other studies [32, 37, 42, 43] using SiO_2 pores were not observed in our experiments. This is likely due to the fact that our nanopores were made with silicon nitride (Si_xN), instead of SiO_2. Recent studies using silicon nitride pores similar to ours have shown that Si_xN nanopores have five times less surface charge density than SiO_2 pores [44]. Thus, the expected crossover salt concentration for the positive spikes would be much lower than 120 mM KCl as reported [43].

3.2 Verification of DNA translocation through a nanopore

Shorter DNA translocations through α-hemolysin channel[17] and solid state nanopores[28] from the *cis* to the *trans* chamber have been verified by gel electrophoresis previously. To demonstrate that the current blockage events corresponded to the translocation of longer DNA molecules via the nanopore, a segment of 1-kbp of dsDNA was prepared by PCR amplification from the PhiX174 genome. The linear 1-kbp dsDNA was then measured in a translocation experiment using a pore with a D_p ~10 nm pore in 1M KCl. After ~40,000 events, the *trans* chamber solution was collected and the sample subjected to 30 rounds of PCR amplification using primers specific for the 1-kbp DNA segment. The PCR sample was analyzed by agarose gel electrophoresis and the result (Fig. S3) showed that the sample

collected from the *trans* chamber was indeed the 1 kbp DNA segment initially placed in the *cis* chamber. Thus, the 1-kbp DNA traversed the nanopore during the translocation experiment (*See* SI.2).

3.3 Effect of KCl concentration on t_{dp}

The most probable peak values of t_{dp} as a function of KCl concentration was plotted as shown in Figure 3A. These data demonstrated that the t_{dp} decreased as KCl concentration was lowered for all the DNA molecules measured. The corresponding open pore currents, I_0, are approximately linearly proportional to the salt concentration within the range of 0.1 to 1M KCl (Fig. S4 in SI), consistent with our earlier work and that of others [30, 43]. As the KCl concentration was decreased, the experimental results in Figures 2 and 3 support the conclusion that the most probable t_{dp} decreased as KCl concentration was lower, and the decrease in t_{dp} varied with the length and conformation of DNA molecules. For the longest λ DNA molecules examined, t_{dp} decreased by more than a factor of 4 as the KCl concentration was lowered from 1M to 0.2M (Fig. 3B).

DNA nanopore electrophoretic mobility and effective charge Q*—The interactions between cations and DNA molecules include: 1) specific cation binding or site-bound, 2) territorially binding of condensed counterions, and 3) the Debye-Huckel type interactions that make the DNA electrical potential go to zero exponentially beyond a characteristic *Debye screening length* [3]. Both specific and territorially binding can reduce a DNA molecule's net charge Q, resulting in a smaller electrophoretic mobility μ ($\propto Q$) that can be observed experimentally. In a monovalent salt solution, the average net charge per phosphate on a DNA molecule, $Q=(1-\theta)q$, is lowered from the elementary charge q by a factor of $(1-\theta)$, θ is the number of associated bound counterions per phosphate (*see* SI.6 for details). For example, Q=0.51q in 0.2M KCl and Q=0.38q in 1M NaCl were estimated by gel electrophoresis [5]. However, for a long DNA molecule with only a fraction of the molecule confined in a ~10 nm nanopore with charged walls, the measured DNA electrophoretic mobility as well as its effective charge is more complicated [45]. Below we attempt to use DNA nanopore electrophoretic mobility μ* and the effective charge Q* to describe the change related to t_d quantitatively. The nanopore electrophoretic mobility μ* is expected to be smaller than its bulk mobility μ by $\mu^* \approx (H_p/L_c)\mu$ due to the fact that only a fraction, H_p/L_c, of a DNA chain is in the pore [46]. Here L_c is the chain length of a DNA molecule.

An increase in μ* or Q* would lead to a shorter t_d—As KCl concentration was lower, the number of bound K^+ ions would be less, leading to a smaller θ and a larger Q *or* a higher electrophoretic mobility μ. Assuming a DNA molecule moves along the central axis of a nanopore, the electric driving force balances the drag force, $\mathbf{F}_E=-\mathbf{F}_{drag}$ [25, 47], and the DNA molecule moves at an average terminal velocity $\bar{v}\approx L_c/t_d=\mu^* E_0$ (for $L_c \gg H_p$). The electric force exerted on the local DNA segment in a pore is $F_E = SQ^* E_0$, here $E_0=\Psi/H_p$ is the electrical field strength and S is the number of phosphates in the pore. The drag force amplitude can be written as $F_{drag} - fv - \eta C_f v$, with $f=\eta C_f$ is the friction coefficient, η *is* the solution viscosity, and C_f is a drag force constant depending on a DNA's conformation and on the parameters not considered here. The time measured is inversely proportion to a DNA molecule's mobility μ* and charge Q* as

$$t_d=\frac{L_c}{\bar{v}}=\left(\frac{L_c}{E_0}\right)\frac{1}{\mu^*}=\left(\frac{L_c}{E_0 S}\right)\frac{\eta C_f}{Q^*}. \quad (1)$$

We use Eq. (1) to emphasize the inverse relationship between t_d with μ^* and Q^* under our experimental conditions. The parameters inside the parenthesis are expected to be constants or to change negligibly as KCl concentration varies. Specifically, $E_0=\Psi/H_p$ was expected to be a constant, and the number of nucleic acids in a pore S was expected to be the same for the same H_p. The chain length L_c has been shown to have negligible dependence on ionic strength in single molecule experiments [48] and is also supported by theory [11]. Furthermore, *an increase in* Q^* at lower KCl concentrations would increase L_{DNA} due to an increase in Coulomb repulsion between bases, this would increase in t_d which would be in the opposite direction as what we observed. Thus, L_{DNA} was unlikely to contribute to the decrease in t_d observed here. We note that the measured t_d has been found to have a nonlinear relationship with DNA chain length L_c, i.e., $t_d \sim L_c^{\alpha}$, where the exponent α was 1.26 [27] and 1.4 [41] for linear DNA molecules, but since L_c remains a constant (the same DNA) for each set of measurements, the rhs of equation (1) holds for any α. The viscosity η in bulk solution had been shown to increase slightly when KCl concentration was lower [49]. Therefore, we do not anticipate that η would contribute to the reduction of t_d as KCl concentration was decreased.

Electro-osmotic flow effects—The simple model used to derive Eq. (1) has ignored many complex issues involved in DNA translocation such as electro-osmotic flow. For a negatively charged DNA molecule passing through a pore with a negatively charged surface, electro-osmotic flow would act to increase t_d which has been used to explain that translocation times vary little with salt concentration [43, 47] in SiO_2 nanopores. In addition, surface charge effects from a nanopore wall would increase at lower salt due to a longer Debye screening length, 0.3 nm (in 1M KCl) to 1 nm (in 0.1M KCl), which would further increase t_{dp} compared with higher salt concentrations [47].

In summary, we conclude that a shorter t_d measured at lower KCl concentration suggests an increase in DNA electrophoretic mobility μ^* or in DNA net charge Q^* or a decrease in C_f. Below we discuss whether the change in Q^* could account for all the change in t_d measured in Figure 3.

The change in Q* could not account for all the change in t_d^{1M}/t_d—Comparing the ratio of t_d^{1M}/t_d as a function of KCl concentration (Fig. 3B), the plots suggest that the ratio of t_d^{1M}/t_d increased as the KCl concentration was lower, but the amount of increase depends on the DNA length and conformation. With the ~10 nm size pores, the ratio of $t_d^{1M}/t_d^{0.2M}$ (or $\mu^*_{0.2M}/\mu^*_{1M}$)=1.5, 1.9, 4.5 for the circular ~22.5kbp, supercoiled 4.4 kbp, and the 48.5 kbp λ DNA, respectively. The effective charge Q^* per phosphate and viscosity η were expected to vary the same amount as KCl concentration was varied from 1M to 0.2 M, thus the large mobility variations suggest that the drag force constant C_f depended on the conformation and length of DNA molecules. In addition, using the same pXba DNA, the ratio of t_d^{1M}/t_d was greater when the measurement was performed with a larger nanopore (~25 nm) (see Fig. 3).

The much larger effect of KCl concentration on λ DNA translocation times must be due to its long length, ~ 16 μm. Considering the length of the local translocating segment of a DNA molecule in a pore is H_p (Fig. 1A), the same regardless its chain length outside the pore, the configuration and motion of the chain outside the pore, such as unwinding upon entering, must be responsible for the greater KCl concentration effect on t_d of λ DNA. Recent theoretical studies have shown that the transport of DNA through pores is controlled by entropic barriers that accompany their conformational changes [50]. However, the conformation and motion of the DNA chain outside a pore and how it affects t_d is beyond the scope of this paper.

In conclusion, the variations in the ratio of t_d^{1M}/t_d for the DNA molecules shown in Fig. 3 suggest that the effective charge Q^* is not the only parameter that affects the t_d, the other parameters such as DNA chain length, conformation, and nanopore size may all contribute to t_d.

3.4 KCl concentration on DNA Conformation

The plots of the instantaneous distribution of ΔI_b in 5-μs samples over all events (Fig. 4) show possible DNA configurations measured in nanopores [25, 51]. The quantified blockage currents of N=1 and N=2 peaks at 1.0 M (Fig. 4A) and 0.2 M (Fig. 4B) correspond to one and two strands of λ dsDNA helices in a pore. At 1M KCl, the ratio of DNA at N=2 versus N=1 is 11:16, or 41% DNA molecules in the N=2 conformation (Fig. 4A). In 0.2M KCl, the ratio is 1:10, or only ~9% of the DNA molecules in the N=2 conformation. The much smaller N=2 peak at 0.2 M KCl suggests that the frequency at which a λ DNA molecule was in folded translocation configuration was less favorable.

For the circular supercoiled pXba DNA in 1.0 M (Fig. 4C) and 0.2 M KCl (Fig. 4D), the quantified blockage currents N=2 and N=4 correspond to two and four strands of dsDNA helices in a pore. The N=4 peak represents DNA molecules in a branched form at 0.2 M KCl that was smaller compared to the same peak in 1M KCl. However, the reduction in the N=4 peak was not as significant as measured for the linear λ DNA.

DNA molecules are less likely to be in folded form at lower KCl concentration—The folding state of a DNA molecule in a nanopore could be caused by either a pre-existing conformation that was captured, or a forced folding or bending by the electric force at the entrance of a nanopore [25]. At low salt concentrations, the reduced probability of detecting DNA in a folded configuration suggested that a DNA molecule had fewer pre-existing folded states or was less bendable by the electric force from the pore as the translocation started. This observation is consistent with other experimental and theoretical studies demonstrating that as the concentration of cations surrounding the DNA decreases, the number of binding counterions to DNA reduces, causing an increase in its effective charge, leading to an increase in its electrophoretic mobility and persistence length [11, 38, 48, 52]. An increase in persistence length, from ~35nm (c=1M) to ~55nm (c=0.1M) [52], would reduce the probability of DNA forming pre-existing folded states and also would be less likely to be bent at the nanopore entrance by an electrical force of the same magnitude (same voltage was applied), which is consistent with our observations (Fig. 4). At higher salt concentrations, due to increased counterion screening, a supercoiled DNA molecule will adopt a highly compact form with more winding and branching than at lower ionic screening [38, 53].

3.5 DNA in more tightly bound Na^+ and Mg^{2+} solution

To further evaluate how cation binding would affect DNA translocation, we performed two more sets of experiments maintaining all of the previous parameters except: 1) K^+ was replaced with Na^+; and 2) adding of low concentrations of Mg^{2+} to the KCl solution.

3.5.1 Replacement of K^+ with Na^+—In a 1M NaCl solution, the open pore current I_0 and the current drop ΔI_b were both modified by the solution conductivity due to the mobility of Na^+ that was reported as 5.19×10^{-4} (cm/s)/(V/cm) in contrast to that of K^+ reported as 7.62×10^{-4} (cm/s)/(V/cm) [54]. For a ~12 nm diameter nanopore, the I_0 was 9.5 nA for 1M KCl. A 3 kbp linear dsDNA (pSP65) was added to the *cis* chamber. After ~ 5,000 events were recorded, both *cis* and *trans* chambers were extensively flushed with 1M NaCl. The I_0 was 7.1 nA for the 1M NaCl solution as expected. The current blockage histograms (Fig. S5A, SI) showed the peak values are ΔI_b=105 ± 16 pA for KCl and ΔI_b=80 ± 17 pA for

NaCl. Histograms of the translocation times (Fig. S5B, SI) showed the peak values are t_d = 90 ± 17 μs in KCl and t_d = 135 ± 16 μs in NaCl. That is, $t_d^{Na+}/t_d^{K+}=\mu^*_{K+}/\mu^*_{Na+}=135/90=1.5$.

In summary, keeping all other parameters the same except for replacing K^+ with Na^+, a longer t_d was measured. These experiments demonstrated that the change in t_d was due to the difference in metal ion binding and suggested that Na^+ ions bind to DNA molecules more tightly resulting in a smaller Q^* and an increased t_d, consistent with reports from bulk based measurements. The change in t_d and in ΔI_b observed here are also consistent with recent published nanopore experimental and simulation results [14]. We can estimate the change in Q* using $t_d \sim \eta/Q^*$ (Eq. 1) by assuming the difference in the drag force constant C_f in 1M NaCl versus 1M KCl was negligible. To correct the viscosity difference, the viscosity of these two salt solutions was measured with a GV-2100 (Gilmont Instruments) ball drop viscometer. The measurements showed that the viscosity of the NaCl solution was 10% greater than the KCl solution, in agreement with interpolated published data [55, 56]. That is: $t_d^{Na+}/t_d^{K+}=(1.1/Q^*_{Na})/(1/Q^*_K)=1.5$ A value of $Q^*_{Na}/Q^*_K=73\%$ is calculated. This relative decrease in Q^* for the 3 kpb DNA in NaCl versus KCl is very close to the reported values for DNA in 0.2 M NaCl versus 0.2 M KCl, Q_{Na}/Q_k = 0.38/0.51=75% was measured by bulk electrophoresis [5].

3.5.2 DNA in more tightly bound Mg^{2+}—We initially attempted to use the 3 kbp linear DNA to evaluate the effect of $MgCl_2$ addition; however, these studies resulted in blocking of the nanopores at $MgCl_2$ concentration above 10 mM [57]. Thus, a 4.4 kbp circular supercoiled DNA (pBR322) was used for the measurements. The experiment was first performed in 1.6 M KCl solution with 10 mM Tris (pH=7.5), 20% glycerol (its electrical conductivity equivalent to 1M KCl) and 0 mM Mg^{+2}. The same solution with 10, 20, 45, and 100 mM $MgCl_2$ was subsequently exchanged in the chambers and the same experiment was performed. The open pore current I_0 and the current blockades ΔI_b were approximately the same, regardless of Mg^{+2} concentration. The peak values in solution from 0 mM Mg^{+2} (Fig. 5A) to 100 mM Mg^{+2} (Fig. 5B) were ΔI_b=210 ± 11 pA representing nicked circular DNA as reported previously [27]. The translocation time, t_{dp}, was increased from 110 ± 5 μs (at 0 mM Mg^{+2}) to 145 ± 11 μs (at 100 mM Mg^{+2}), a 32% increase in t_d (Fig. 5c). The increase in t_d was consistent with early reports that divalent ion Mg^{2+} binds to DNA more tightly than the monovalent ion K^+, and adding divalent salt $MgCl_2$ to a KCl solution would further reduce the net charge Q^* and mobility μ of the DNA [7, 11].

The increase in t_d: During the above set of measurements, the only variable was the addition of $MgCl_2$ (≤100 mM) to the KCl solution. The more tightly bound Mg^{+2} ions would further decrease the effective charge Q^* as well as the mobility μ^* of the DNA molecules [7, 9, 58], resulting in a longer t_d as we observed. All parameters, including V, L_{DNA}, N, S, C_f, η, except Q^* in Eq. (1) can be considered as constants or would not contribute to the increase in t_d. The difference in viscosities for a small salt concentration change (≤100 mM) is negligible if interpolated from published data [55]. As the Q^* decreases, its length (L_{DNA}) was expected to be shorter due to a decreased Coulomb repulsion, thus, L_{DNA} was unlikely to contribute to the increase in t_d. Therefore, the change in Q* can be estimated from Eq. (1) by $t_d \sim 1/Q^*$. For example, at 100mM Mg^{+2}, the ratio of t_d^{100mM}/t_d^0=1.32 (Fig. 5C, right). Here t_a^0 is the translocation time at 0 mM Mg^{+2}. Using $t_d^{100mM}/t_d^0=Q^0/Q^{100mM}$, the estimated DNA net charge is $Q^{100mM}=0.76Q^0$. In other words, these results show that adding Mg^{+2} ions can further neutralize a DNA's charge or decrease its mobility in a KCl solution.

An increase in N=4 conformation: The plots of the distribution of instantaneous ΔI_b samples over all events (Fig. 5D) show that the current blockage levels occurred in integer multiples, and the frequency of N=4 configuration increased as more Mg^{+2} ions were added. At 100 mM Mg^{+2} (Fig. 5D) the supercoiled DNA had more N=4 configurations inside the nanopore as compared to the absence of Mg^{+2}. These results indicate that the supercoiled DNA molecules were more branched or more bendable as more Mg^{+2} ions were added. As the Mg^{+2} concentration increases, the increased counterion screening would further reduce DNA effective charge Q^* that could cause a supercoiled DNA molecule to become more tightly wound; eventually winding tightly enough to produce a greater number of branched supercoiled DNA molecules [59–61]. It was also possible that a decrease in the net charge made a DNA molecule be more bendable at the entrance of a nanopore.

Notes: limits of this study: The study of chloride salts on DNA translocation in silicon nitride nanopores described in this work was limited by several factors. First, at salt concentrations lower than 0.1 M, the current drop was too small to be measured accurately. Second, divalent and trivalent counterions bind to DNA molecules more tightly than monovalent ions, having a greater screening of electrostatic charge causing the DNA to precipitate out of solution. The attempts to measure DNA in divalent ion salts alone, Mg^{+2} and Ca^{+2}, as well as trivalent ions Al^{+3} and $Co(NH_3)_6^{+3}$ were not successful due to DNA precipitation, indicating the limitations to increasing DNA translocation time by reducing DNA net charge or increasing counterion binding. Lastly, the silicon nitride nanopores often became unusable (a change of I_0 or too noisy) before a complete set of experiments could be performed.

Concluding Remarks

At single molecule level, we have studied how KCl concentration and metal ion binding affects DNA translocation through solid state nanopores. DNA molecules representing different forms, including linear, circular, and supercoiled, and with wide range of lengths from ~1 μm to ~16.5 μm were measured in this work. As the ionic strength was increased, our nanopore measurements showed that DNA molecules became more folded or branched and their translocation times in a nanopore were longer. By analyzing how the relative DNA translocation times changed as a function of KCl concentration, our results suggest that the change in DNA effective charge due to counterion screening played important roles in DNA translocation dynamics, however, other parameters such as DNA length, conformation, as well as nanopore size also contributed significantly. Moreover, our studies indicate that Na^+ is more effective at screening DNA charge than K^+, and adding Mg^{+2} to a KCl solution can further neutralize the charge of DNA molecules. The studies in this work will improve our understanding of nanopore-based DNA sensing and on DNA-counterion binding at single molecule level.

Supplementary Material

Refer to Web version on PubMed Central for supplementary material.

Acknowledgments

The authors thank Professor J. Golovchenko for FIB pore preparation, Dr. Slaven Garaj for helpful discussion, John Wang for Matlab programming, and Bradley Ledden for nanopore fabrication. Support of this research has been provided by NIH R21HG003290, NIH R21HG004776, ABI1114, and partially supported by NSF/MRSEC 080054.

A list of abbreviations used in the paper

SI	Supporting Information
TE buffer	10 mM Tris at pH 7.5 with 1 mM EDTA

References

1. Sigel H. Chem Soc Rev. 1993; 22:255–267.
2. McFail-Isom L, Sines CC, Williams LD. Current Opinion in Structural Biology. 1999; 9:298–304. [PubMed: 10361089]
3. Bloomfield, VA.; Crothers, DMI.; Tinoca, J. Nucleic Acids: structures, properties, and functions. University Science Books; 1999. p. 475-534.
4. Tan ZJ, Chen SJ. Biophys J. 2006; 90:1175–1190. [PubMed: 16299077]
5. Ross PD, Scruggs RL. Biopolymers. 1964; 2:231–236.
6. Rhee KW, Ware BR. J Chem Phys. 1983; 78:3349–3353.
7. Li AZ, Huang H, Re X, Qi LJ, Marx KA. Biophys J. 1998; 74:964–973. [PubMed: 9533707]
8. Stellwagen E, Stellwagen NC. Biophys J. 2003; 84:1855–1866. [PubMed: 12609887]
9. Ahmad R, Arakawa H, Tajmir-Riahi HA. Biophys J. 2003; 84:2460–2466. [PubMed: 12668453]
10. Feig M, Pettitt BM. Biophys J. 1999; 77:1769–1781. [PubMed: 10512802]
11. Manning GS. Q Rev Biophys. 1978; 2:179–246. [PubMed: 353876]
12. Manning GS. J Phys Chem. 1981; 85:1506–1515.
13. Luan B, Aksimentiev A. Phys Rev E. 2008:78.
14. Kowalczyk SW, Wells DB, Aksimentiev A, Dekker C. Nano Lett. 2012; 12:1038–1044. [PubMed: 22229707]
15. Oukhaled G, Bacri L, Mathe J, Pelta J, Auvray L. Europhys Lett. 2008:82.
16. Reiner JE, Kasianowicz JJ, Nablo BJ, Robertson JWF. PNAS. 2010; 107:12080–12085. [PubMed: 20566890]
17. Kasianowicz JJ, Brandin E, Branton D, Deamer DW. Proc Natl Acad Sci USA. 1996; 93:13770–13773. [PubMed: 8943010]
18. Akeson M, Branton D, Kasianowicz JJ, Brandin E, Deamer DW. Biophys J. 1999; 77:3227–3233. [PubMed: 10585944]
19. Meller A, Nivon L, Brandin E, Golovchenko J, Branton D. Proc Natl Acad Sci USA. 2000; 97:1079–1084. [PubMed: 10655487]
20. Gu LQ, Braha O, Conlan S, Cheley S, Bayley H. Nature. 1999; 398:686–690. [PubMed: 10227291]
21. Nakane J, Wiggin M, Marziali A. Biophys J. 2004; 87:615–621. [PubMed: 15240494]
22. Astier Y, Braha O, Bayley H. J Am Chem Soc. 2006; 128:1705–1710. [PubMed: 16448145]
23. Clarke J, Wu H, Jayasinghe L, Patel A, et al. Proc Natl Acad Sci USA. 2009; 106:7702–7707. [PubMed: 19380741]
24. Li J, Stein D, McMullan C, Branton D, et al. Nature. 2001; 412:166–169. [PubMed: 11449268]
25. Li J, Gershow M, Stein D, Brandin E, Golovchenko JA. Nat Mater. 2003; 2:611–615. [PubMed: 12942073]
26. Storm AJ, Chen JH, Ling XS, Zandbergen HW, Dekker C. Nat Mater. 2003; 2:537–540. [PubMed: 12858166]
27. Storm AJ, Chen JH, Zandbergen HW, Dekker C. Phys Rev E. 2005; 71:0519031–05190310.
28. Heng JB, Ho C, Kim T, Timp R, et al. Biophys J. 2004; 87:2905–2911. [PubMed: 15326034]
29. Fologea D, Gershow M, Ledden B, McNabb DS, et al. Nano Lett. 2005; 5:1905–1909. [PubMed: 16218707]
30. Fologea D, Uplinger J, Thomas B, McNabb DS, Li J. Nano Lett. 2005; 5:1734–1737. [PubMed: 16159215]
31. Gershow M, Golovchenko JA. Nat Nanotechnol. 2007; 2:775–779. [PubMed: 18654430]

32. Peng H, Ling XS. Nanotechnology. 2009; 20
33. Venkatesan BM, Shah AB, Zuo JM, Bashir R. Adv Funct Mater. 2010; 20:1266–1275. [PubMed: 23335871]
34. Singer A, Wanunu M, Morrison W, Kuhn H, et al. Nano Letters. 2010; 10:738–742. [PubMed: 20088590]
35. Wanunu M, Dadosh T, Ray V, Jin J, et al. Nat Nano. 2010; 5:807–814.
36. Wanunu M, Sutin J, McNally B, Chow A, Meller A. Biophys J. 2008; 95:4716–4725. [PubMed: 18708467]
37. Dorp, Sv; Keyser, UF.; Dekker, NH.; Dekker, C.; Lemay, SG. Nat Phys. 2009; 5:347–351.
38. Schlick T, Li B, Olson WK. Biophys J. 1994; 67:2146–2166. [PubMed: 7696459]
39. Stein DM, McMullan CJ, Li J, Golovchenko JA. Rev Sci Instrum. 2004; 75:900–905.
40. Cai Q, Ledden B, Krueger E, Golovchenko JA, Li J. J Appl Phys. 2006:100.
41. Fologea D, Brandin E, Uplinger J, Branton D, Li J. Electrophoresis. 2007; 28:3168–3192.
42. Chang H, Kosari F, Andreadakis G, Alam MA, et al. Nano Lett. 2004; 4:1551–1556.
43. Smeets RM, Keyser UF, Krapf D, Wu MY, et al. Nano Lett. 2006; 6:89–95. [PubMed: 16402793]
44. Hoogerheide DP, Garaj S, Golovchenko JA. Phys Rev Lett. 2009:102.
45. Keyser UF, van Dorp S, Lemay SG. Chem Soc Rev. 2009; 39:939–947. [PubMed: 20179816]
46. Li J, Talaga DS. J Phys Condens Matter. 2010; 22:454129, 454128. [PubMed: 21339615]
47. Ghosal S. Phys Rev Lett. 2007:98.
48. Baumann CG, Smith SB, Bloomfield VA, Bustamante C. Proc Natl Acad Sci USA. 1997; 94:6185–6190. [PubMed: 9177192]
49. Brown WR, Yousef HNS. J Colloid Interface Sci. 2003; 264:452–457. [PubMed: 16256664]
50. Muthukumar M. Annu Rev Biophys Biomol Struct. 2007; 36:435–450. [PubMed: 17311526]
51. Storm AJ, Storm C, Chen J, Zandbergen H, et al. Nano Lett. 2005; 5:1193–1197. [PubMed: 16178209]
52. Manning GS. Biophys J. 2006; 91:3607–3616. [PubMed: 16935960]
53. Anderson P, Bauer W. Biochemistry. 1978; 17:594–601. [PubMed: 623732]
54. Hille, B. Ion Channels of Excitable Membranes. Sinauer Associates, Inc; Sunderland, MA: 2001.
55. Weast, RC., editor. CRC Handbook of Chemistry and Physics, 1985–1986. CRC Press, Inc; Boca Raton, FL: 1985.
56. Nickels L, Allmand AJ. J Phys Chem. 1936; 41:861–872.
57. Bloomfield VA. Curr Opin Struct Biol. 1996; 6:334–341. [PubMed: 8804837]
58. Korolev N, Lyubartsev AP, Rupprecht A, Nordenskiold L. Biopolymers. 2001; 58:268–278. [PubMed: 11169387]
59. Bendar J, Furrer P, Stasiak A, Dubochet J. J Mol Biol. 1994; 235:825–847. [PubMed: 8289322]
60. Fogg JM, Kolmakova N, Rees I, Magonov S, et al. J Phys Condens Matter. 2006; 18:S145–S159. [PubMed: 19337583]
61. Xu YC, Bremer H. Nucleic Acids Res. 1997; 25:4067–4071. [PubMed: 9321659]

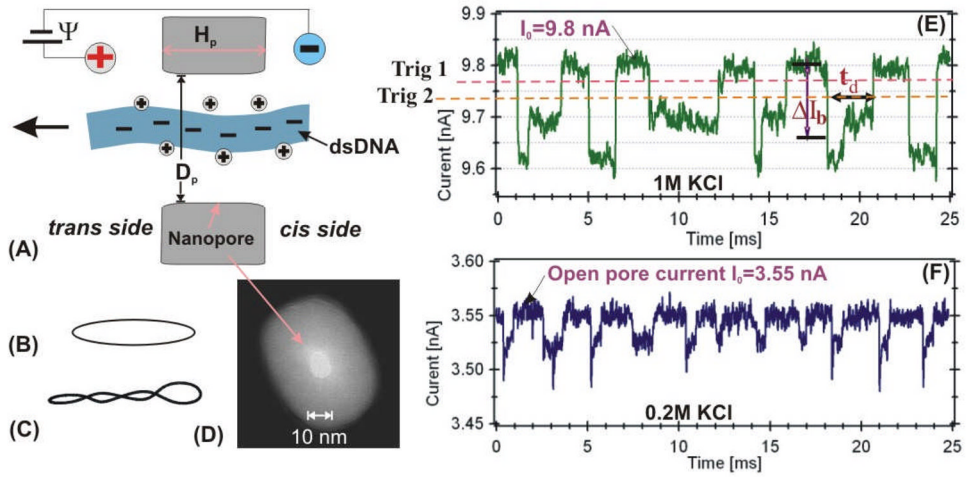

Figure 1.

Schematic of a linear DNA molecule translocating through a nanopore (A). Other conformations of DNA measured in this work: circular relaxed (B) and circular supercoiled (C). TEM image of a ~10-nm silicon nitride nanopore (D). Examples of current blockage events for λ DNA measured in 1M KCl (E) and 0.2 M KCl (F) with the ~10 nm pore shown in (D).

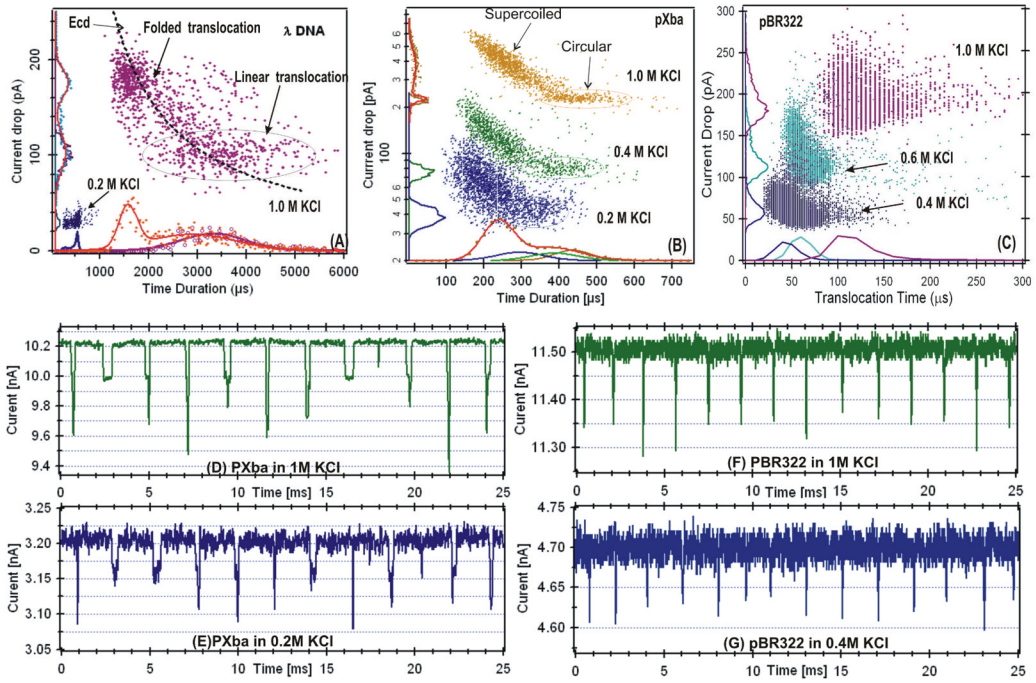

Figure 2.

Event distribution plots for: (A) linear λ DNA in 1M and 0.2M KCl, (B) a mixture of circular and supercoiled 22.5 kbp DNA, and (C) supercoiled 4.4 kbp DNA. A separate nanopore was used for the data shown in each panel. Examples of the time histograms of these measurements are shown on the bottom axis. More examples of current blockage events are shown for pXba in 1M KCl (D) and in 0.2M KCl (E), for PBR322 in 1M KCl (F) and in 0.4M KCl (G). For the pBR322 4.4 kbp DNA data recording, **t**he low pass Bessel filter in the Axopatch 200B was set to 100 kHz.

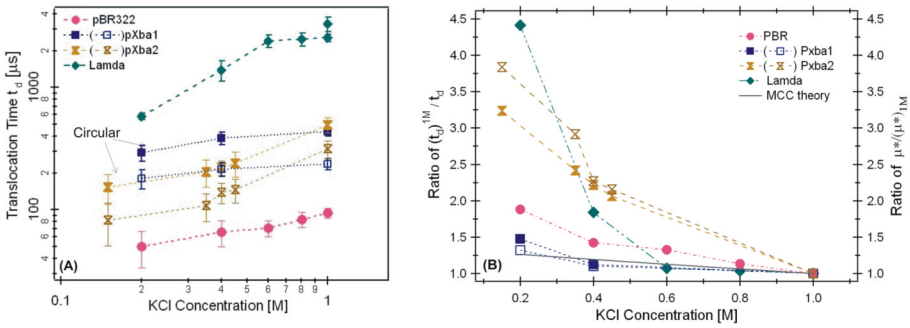

Figure 3.

(A) The most probable peak values t_{dp} measured as a function of KCl concentration. The filled square (■) is for the circular and the unfilled square (□) is for the supercoiled pXba measured in a ~10 nm pore. The filled hourglass (⧗) is for the circular and the unfilled hourglass (⧖) is for the supercoiled pXba measured in a ~25 nm pore. (B) The ratio of t_d^{1M}/t_d for the DNA molecules measured in (A). The solid line is the theoretically predicted change from MCC theory (see SI.5).

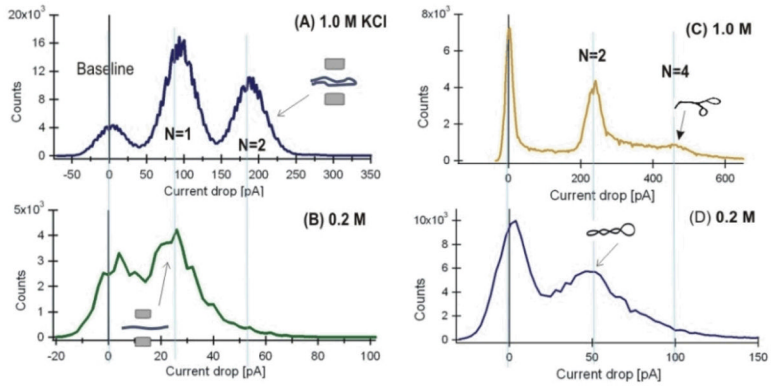

Figure 4.

The distribution of 5-μs current samples per 2 pA bin of ΔI_b at 1 M and 0.2 M KCl. (A) and (B) are for λ DNA data shown in Figure 2A, the insets show the assumed DNA translocation configurations for N=1 and N=2. (C) and (D) are for the supercoiled events of the pXba DNA in Fig. 2B. The baseline peaks at 0 pA corresponds to the open pore level (I_0).

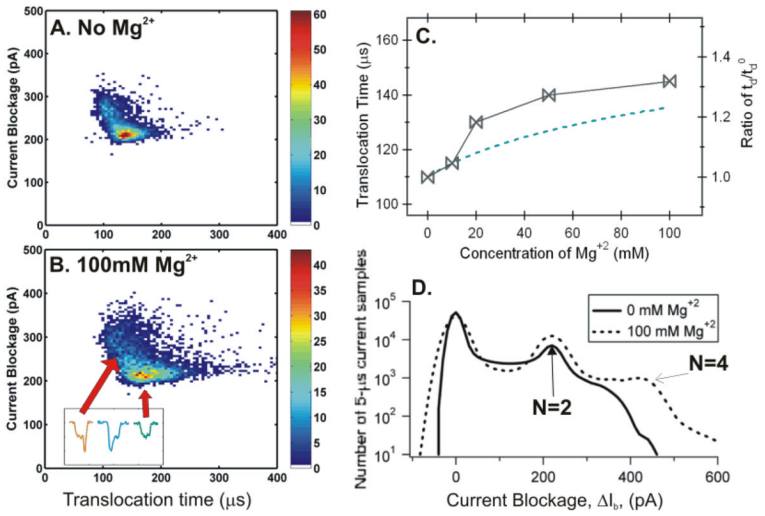

Figure 5.

Event number density plots for (A) 0 mM and (B) 100 mM Mg^{+2} in TE buffer with 20% glycerol. The insert in Fig. 5B shows three events, one corresponding to a circular DNA and the other two corresponded to branched or bent supercoiled DNA. (C) Left, t_d as a function of the amount of Mg^{+2} ions added. Right, the change in t_d/t_d^0. The Dashed line is the theoretically predicted values from MCC theory (see SI.4.). (D) Histograms of the number of 5-μs current blockage samples per 2 pA bin for 0 and 100 mM Mg^{+2}. A ~14 nm pore was used with I_0 = 11.25 nA.

Table 1

The t_{dp} and ΔI_{bp} values for all DNA molecules measured at all KCl concentrations.

KCl [M]	λ DNA		pXba1				pXba2				pBR322	
	Linear		Circular		Super coiled		Circular		Super coiled			
	t_d [μs]	ΔI_b[pA]/I_0[nA]	t_d [μs]	ΔI_b[pA]/I_0[nA]	t_d [μs]	ΔI_b[pA]/I_0[nA]	t_d [μs]	ΔI_b[pA]/I_0[nA]	t_d [μs]	ΔI_b[pA]/I_0[nA]	t_d [μs]	ΔI_b[pA]/I_0[nA]
0.15							153 ± 42	32/7.0	82 ± 27	38/7.0		
0.2	568 ± 37	28/3.55	294 ± 45	42/3.2	180 ± 30	58/3.2					50 ± 16	29.6/2.7
0.35							205 ± 52	37/14.4	108 ± 28	47/14.4		
0.4	1394 ± 270	39/4.65	386 ± 46	79/5.7	214 ± 51	110/5.7	223 ± 30	37/16.6	139 ± 26	47/16.6	66 ± 16	51.5/4.7
0.45							240 ± 56	44/18.3	147 ± 32	53/18.3		
0.6	2390 ± 275	73/5.4									71 ± 10	102.1/6.7
0.8	2480 ± 310	81/6.7									83 ± 12	111.4/9.2
1.0	2944 ± 645	104/**9.8**	434 ± 34	220/**10.3**	237 ± 31	315/**10.3**	495 ± 70	79/36.9	316 ± 53	104/36.9	94 ± 8	179.6/**11.5**